Charge Separation

DOI: 10.1002/anie.200604483

Extremely Stable Photoinduced Charge Separation in a Colloidal System Composed of Semiconducting Niobate and Clay Nanosheets**

*Nobuyoshi Miyamoto, Yoshimi Yamada, Satoshi Koizumi, and Teruyuki Nakato**

Colloidal semiconductor particles have been investigated because of their applications in photoenergy conversion and photocatalysis.[1] Electrons and holes generated upon bandgap photoexcitation of the semiconductor particles are separated by subsequent interfacial electron transfer to acceptor and donor molecules. The stabilization of the charge-separated state is key for controlling the photochemical reactions induced by photoexcitation of the semiconductor particles.

The spatial separation of the acceptor and donor species can be used effectively to stabilize the charge-separated state by suppressing back electron transfer. Heterogeneous media, such as micelles and vesicles, have been utilized for such purposes;[2] for example, the photoinduced charge separation between semiconducting particles and acceptor or sensitizer molecules has been achieved by using vesicles,[3] microemulsions,[4] and SiO_2 particles[5] as the heterogeneous media. However, in these colloidal systems the photogenerated charge-separated states are still short-lived (with lifetimes of only a few minutes). The incorporation of acceptor and donor components into nanostructured solids, such as layered[6,7] and porous materials,[8] stabilizes effectively the charge-separated state (with lifetimes of up to several hours). Nevertheless, solid systems have a drawback regarding the difficulty of being penetrated by both light and molecules. Another disadvantage is that the charge-separated products which store the photoenergy cannot undergo further reactions easily.

In this context, we have explored another method for combining semiconductor particles and acceptor species into a superstructure, thereby producing a stable photoinduced charge-separated state with diffusiveness of molecules. To select the colloidal semiconducting particles, we turned our attention to inorganic nanosheets obtained by exfoliation of layered semiconducting materials (exemplified by niobates and titanates).[9] These semiconducting nanosheets have a peculiar two-dimensional morphology (with a thickness of 1–2 nm and a lateral size of up to 100 μm), which leads to the formation of various superstructures[10] with photoactive properties akin to those of bulk TiO_2.[11] Recently, the self-assembly of colloidal particles into superstructures was investigated. Anisotropic colloidal particles can be organized into lyotropic liquid crystals[12,13] (similar to the way in which spherical particles form colloidal crystals).[14] Multicomponent colloids—which contain more than two kinds of particles with different size, shape, and physical properties—form a rich variety of superstructures by (micro)phase separation.[15] In addition, mixing inorganic nanosheets with a lamellar-micelle surfactant phase leads to the formation of microdomain structures.[16] Thus, we expect to obtain colloidal superstructures which are suitable for spatially separating the acceptor and donor species.

Herein, we show that the lifetime of the charge-separated state, initiated by photoexcitation of the semiconductor particles, increases dramatically in a colloidal mixture consisting of two kinds of exfoliated inorganic nanosheets prepared from semiconducting layered niobate and photochemically inert clay (see Figure S1 in the Supporting Information illustrates their structures). Our recent study revealed that mixtures of niobate and clay nanosheets form microdomains with differences in composition and selectivity towards the adsorption of cationic dyes.[17] Such microdomain structures consist of a domain that contains niobate nanosheets (which act as photoactive electron donors) and another one in which clay nanosheets are present. These clay nanosheets selectively adsorb the cationic electron acceptor methylviologen (MV^{2+}; see the molecular structure in Figure S1c of the Supporting Information). The spatial separation between the electron donor (namely, niobate) and the acceptor (namely, the MV^{2+} ions adsorbed on clay) results in the charge-separated state initiated by UV irradiation remaining stable.

The presence of the stable radical ion $MV^{+\bullet}$, which is formed by electron transfer to MV^{2+} ions, characterizes the long-lived charge separation induced by UV irradiation of a mixture of niobate and hectorite colloids doped with MV^{2+} ions (represented hereafter as MV/hectorite–niobate colloids). In the visible spectra of an MV/hectorite–niobate

[*] Y. Yamada, Prof. T. Nakato
Division of Bio-Applications and Systems Engineering (BASE)
Institute of Symbiotic Science and Technology
Tokyo University of Agriculture and Technology
2-24-16 Naka-cho, Koganei-shi, Tokyo 184-8588 (Japan)
Fax: (+81) 42-388-7344
E-mail: tnakat@cc.tuat.ac.jp
Dr. N. Miyamoto, Prof. T. Nakato
PRESTO, Japan Science and Technology Corporation (JST)
Saitama 332-0012 (Japan)
Dr. N. Miyamoto, Dr. S. Koizumi
Advanced Science Research Center
Japan Atomic Energy Agency (JAEA)
2-4 Shirakata-Shirane, Tokai-mura, Naka-gun
Ibaraki 319-1195 (Japan)

[**] This work was partly supported by a Grant-in-Aid for Scientific Research (no. 16350107) from the Ministry of Education, Culture, Sports, Science, and Technology, Japan. We thank the referees for their useful comments.

Supporting information for this article is available on the WWW under http://www.angewandte.org or from the author.

colloid (with $[MV^{2+}] = 0.3\,mM$; [hectorite] $= 2.0\,g\,L^{-1}$; and [niobate] $= 2.0\,g\,L^{-1}$), we observe the emergence of a sharp band at 400 nm and a broad one at 607 nm; these signals correspond to the species $MV^{+\bullet}$[18] after UV irradiation (colored solid lines in Figure 1), whereas only a background

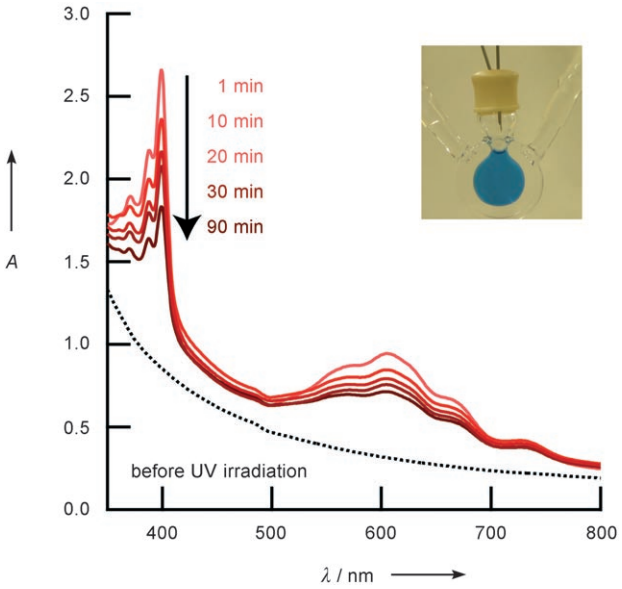

Figure 1. Visible absorption spectra of the MV/hectorite–niobate colloid (with [hectorite] $= 2.0\,g\,L^{-1}$, [niobate] $= 2.0\,g\,L^{-1}$, and $[MV^{2+}] = 0.3\,mM$) before (•••••) and after 5 min of UV irradiation (the light-to-dark red lines correspond to spectra recorded at 1, 10, 20, 30, and 90 min after stopping irradiation). Inset: Photograph of the colloid in the quartz cell after UV irradiation.

curve arising from light scattering of the nanosheets is observed before irradiation (dotted line, Figure 1). The formation of the radical species can also be "seen" as the colloid changes its color—from colorless to blue—upon UV irradiation (inset, Figure 1). The photogenerated $MV^{+\bullet}$ species is very long-lived, as indicated by the absorption bands which remained present for several hours.

An analysis of the decay process of the photogenerated $MV^{+\bullet}$ species quantitatively shows that its lifetime is much longer than that of other colloidal semiconductor systems; we observed an apparent single-exponential decay for the $MV^{+\bullet}$ species (with a time constant τ_d). By fitting the experimental data (Figure 2a, squares), we obtained the value $\tau_d = 11.0$ h for the MV/hectorite–niobate colloid (with $[MV^{2+}] = 0.1\,mM$, [niobate] $= 2.0\,g\,L^{-1}$, and [hectorite] $= 10.0\,g\,L^{-1}$). In a dispersion of semiconductor particles without a heterogeneous medium, the lifetimes of the generated charge-separated states are only several milliseconds.[19] Even in the systems in which the semiconductor particle and the acceptor are separated by vesicle layers, the lifetimes are shorter than an hour.[3] Thus, the charge-separated state generated herein is very long-lived relative to lifetimes reported for other systems.

Not only the slow decay but also the slow generation of $MV^{+\bullet}$ species characterizes the photochemistry of the present

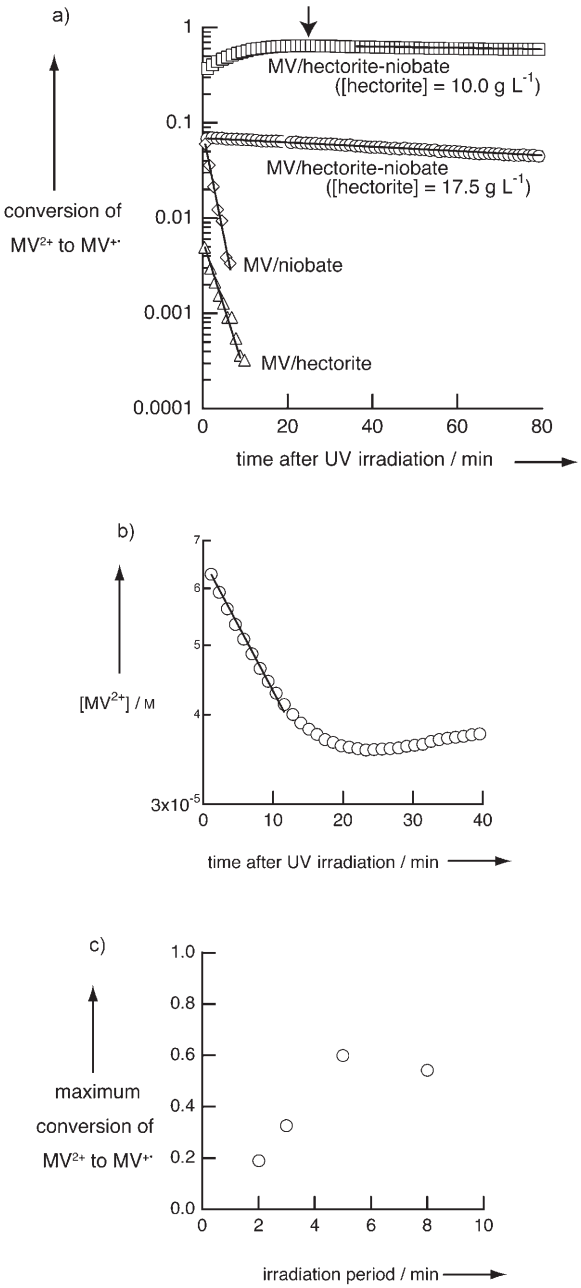

Figure 2. Generation and decay of $MV^{+\bullet}$ monitored by visible spectroscopy. a) Time course of the conversion of MV^{2+} to $MV^{+\bullet}$ in the MV/hectorite–niobate colloid, with [hectorite] $= 10.0$ (□) and $17.5\,g\,L^{-1}$ (○), [niobate] $= 1.0\,g\,L^{-1}$, and $[MV^{2+}] = 0.1\,mM$; the MV/hectorite colloid (△), with [hectorite] $= 2.0\,g\,L^{-1}$ and $[MV^{2+}] = 0.3\,mM$; and the MV/niobate colloid (◇), with [niobate] $= 2.0\,g\,L^{-1}$ and $[MV^{2+}] = 0.3\,mM$, after 5 min of UV irradiation. b) Time course of $[MV^{2+}]$ in the MV/hectorite–niobate colloid (with [hectorite] $= 10.0\,g\,L^{-1}$, [niobate] $= 1.0\,g\,L^{-1}$, and $[MV^{2+}] = 0.1\,mM$) after stopping the UV irradiation. c) Irradiation-period dependence of the maximum conversion of MV^{2+} ions into $MV^{+\bullet}$ species in the MV/hectorite–niobate colloid (with [hectorite] $= 10.0\,g\,L^{-1}$, [niobate] $= 1.0\,g\,L^{-1}$, and $[MV^{2+}] = 0.1\,mM$). The solid lines in (a) and (b) correspond to a fitting to a single-exponential function. The arrow in (a) indicates the maximum conversion of MV^{2+} ions into $MV^{+\bullet}$ species.

MV/hectorite–niobate colloids. Generation of $MV^{+\bullet}$ species continues even after stopping the UV irradiation (Figure 2a,

squares). We found that the conversion of MV^{2+} into $MV^{+\bullet}$ obeys a single-exponential time function with a time constant τ_g. By fitting the data (Figure 2b), we obtained $\tau_g = 0.4$ h for the colloid with [hectorite] = 10.0 g L^{-1}. A slower generation of the charge-separated state was observed in the systems in which the donor and acceptor sites were spatially separated and a mediator species shuttled the electrons between them by slow diffusion.[20] In our case, the niobate nanosheets themselves should shuttle electrons between the domains, thus resulting in a slower generation of the charge-separated state.

In our system, the $MV^{+\bullet}$ species are efficiently generated by UV irradiation, since τ_d is much larger than τ_g. The maximum conversion efficiency of MV^{2+} into $MV^{+\bullet}$ is evaluated from the time course of [$MV^{+\bullet}$] after UV irradiation (see Figure 2a). This efficiency reaches 60% at 25 minutes after irradiation of the colloids with [hectorite] = 10.0 g L^{-1} (indicated by the arrow). As shown in Figure 2c, we also found that the maximum conversion depends on the irradiation period (that is, it increases with the irradiation period until saturation occurs at around 5 min). This fact is attributed to an increase in the amount of absorbed photons with longer irradiation periods and confirms that the formation of $MV^{+\bullet}$ species is initiated by UV light.

Control experiments indicate that the long-lived $MV^{+\bullet}$ species is generated only when both niobate and hectorite coexist in the colloid. In the single-component niobate (Figure 3a) or hectorite (Figure 3b) colloids doped with MV^{2+} ions (and denoted hereafter as MV/niobate and MV/hectorite), only weak bands emerge in the visible spectra after UV irradiation. These bands are assigned to photogenerated $MV^{+\bullet}$ species.[7,21] However, the amount of generated $MV^{+\bullet}$ species is very small and the radical ions disappear within several minutes (diamonds and triangles in Figure 2a). Furthermore, the amount of $MV^{+\bullet}$ species generated in MV/niobate decreases considerably upon prolonged UV irradiation because of photocatalytic decomposition by the semiconducting niobate nanosheets.[22] The prevention of photocatalytic decomposition in the MV/hectorite–niobate samples indicates that the MV^{2+} species are held apart from the niobate nanosheets when clay nanosheets coexist in the colloid (as described in the following paragraphs).

We explored the structure of the MV/hectorite–niobate colloids, which should be key for the generation of long-lived radical ions. In the visible spectra, the absorption maxima corresponding to $MV^{+\bullet}$ species were observed at 395, 557, and 602 nm for the MV/niobate colloid (Figure 3a) and at 400 and 607 nm for both the MV/hectorite (Figure 3b) and the MV/hectorite–niobate (Figure 3c) colloids. This fact indicates that the $MV^{+\bullet}$ species are selectively adsorbed on the hectorite nanosheets in the MV/hectorite–niobate colloid, although both hectorite and niobate have cation-exchange capability. The selective adsorption is further confirmed by the transfer of MV^{2+} ions from the niobate nanosheets to the hectorite nanosheets through a cellulose membrane that macroscopically separates both components (see Figure S2 in the Supporting Information). We have already reported a similar selective adsorption of a cationic cyanine dye onto montmorillonite clay in the presence of niobate.[17] The affinity of clay minerals for organic molecules is explained by the hydrophobic nature of their surface siloxane structure.[23]

Small-angle neutron scattering (SANS) measurements of the nanosheet colloids confirm that each of the niobate and clay nanosheets forms microdomains (see Table of Contents). Two peaks appear at $q = 0.12$ and $q = 0.23$ nm^{-1} in the SANS profile of the niobate nanosheet colloid (Figure 4a); these peaks are ascribed to a lamellar structure with a basal spacing of $d = 2\pi/q = 55$ nm (this lamellar structure is attributed to the ordered niobate nanosheets, which are in a liquid-crystalline state because of the excluded-volume effect).[24] At hectorite concentrations of 10.0 and 17.5 g L^{-1} (Figure 4b,c), the peaks

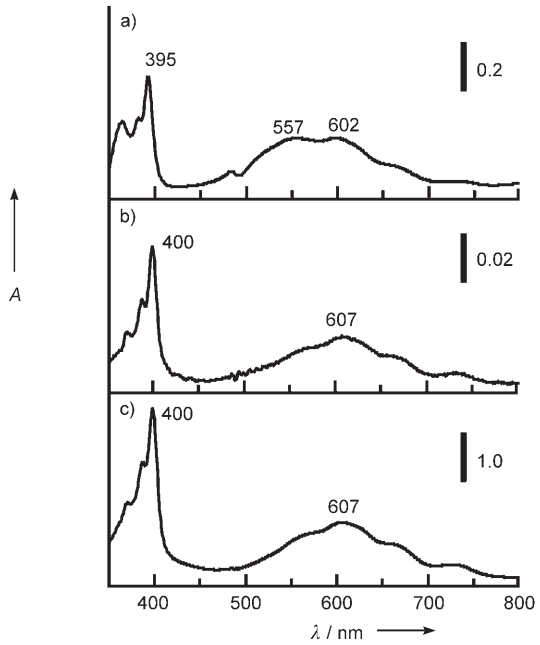

Figure 3. Difference spectra (between the data taken before and after UV irradiation) for the: a) MV/niobate (with [niobate] = 2.0 g L^{-1} and [MV^{2+}] = 0.3 mM), b) MV/hectorite (with [hectorite] = 2.0 g L^{-1} and [MV^{2+}] = 0.3 mM), and c) MV/hectorite–niobate (with [hectorite] = 2.0 g L^{-1}, [niobate] = 2.0 g L^{-1}, and [MV^{2+}] = 0.3 mM) colloids.

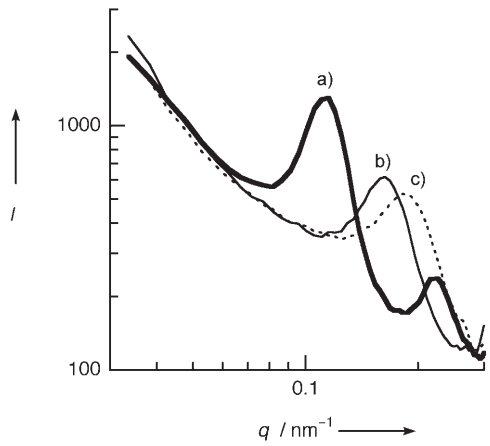

Figure 4. Small-angle neutron scattering (SANS) profiles of hectorite–niobate colloids. The colloids contain 62.0 g L^{-1} of niobate nanosheets and a) 0, b) 10.0, and c) 17.5 g L^{-1} of hectorite nanosheets.

shift to higher q values, that is, the basal spacing decreases to 40 and 35 nm, respectively. This reduction of the basal spacing is interpreted as the formation of hectorite microdomains by means of a microphase separation between the hectorite and niobate nanosheets and a compression of the liquid-crystalline niobate phase by the intruding hectorite phase. In general, phase separation is observed in colloidal mixtures of particles with different sizes and/or shapes.[15,16] This separation is driven by a balance between mixing and translational entropy and/or depletion attraction of the larger components. The emergence of niobate and hectorite domains is feasible because of the large differences in the lateral dimensions of the hectorite (about 20 nm)[25] and niobate ($>1\ \mu m$)[24] nanosheets. The volume fraction of the clay nanosheets in the hectorite–niobate colloids (that is, 0.4 and 0.7 vol% for a colloid concentration of 10.0 and 17.5 $g\,L^{-1}$, respectively) is comparable to that in niobate (namely, 1.7 vol%) and is large enough to cause the structural modifications of the colloid described above. It is unlikely that hectorite nanosheets are homogeneously present in the colloid; the interlamellar spacing between the niobate nanosheets should not decrease if the clay nanosheets behave as solvent molecules.

We presume that the stable charge separation is related to the softness of the microdomain structure. Viscous colloids, in which diffusion of the nanosheets is suppressed, destabilize the charge-separated state. If we increase the hectorite content from 10.0 to 17.5 $g\,L^{-1}$, the sample becomes partly gelated, thus yielding fewer $MV^{+\bullet}$ ions (only 8% conversion) with a shorter lifetime (namely, $\tau_d = 3.2$ h, see Figure 2a, circles). In addition, no slower generation of $MV^{+\bullet}$ species was observed after stopping light irradiation. In this sample, only neighboring niobate and MV/hectorite nanosheets should take part in the photoprocess, since the diffusion of nanosheets is blocked by the gelation. In both systems (with [hectorite] = 10.0 and 17.5 $g\,L^{-1}$), the signal corresponding to the $MV^{+\bullet}$ species decays very fast (within a second) when the colloids are mechanically agitated after UV irradiation. This fact indicates that rapid diffusion of the nanosheets is disadvantageous for maintaining the charge-separated state. Hence, an appropriate softness that allows slow diffusion of the nanosheets is necessary to achieve an effective electron transfer accompanied by a stable charge separation.

We propose the following model for the photoprocesses in the MV/hectorite–niobate colloid: Upon UV irradiation, the niobate nanosheets are excited to generate electron–hole pairs (with the electrons remaining in the conduction band of the nanosheets). Then, $MV^{+\bullet}$ species are yielded by means of a transfer of the photoexcited electrons from the niobate nanosheets to the MV^{2+} ions adsorbed on the hectorite nanosheets. The formation of $MV^{+\bullet}$ species should take place at the interface between the hectorite and the niobate microdomains. Since the diffusion of the nanosheets that form the microdomains is slower than that of the molecular species, the generation of $MV^{+\bullet}$ species is slowed. Finally, the generated $MV^{+\bullet}$ species are slowly oxidized to MV^{2+} ions. The recovery of MV^{2+} ions is demonstrated by repeated irradiation of the MV/hectorite–niobate colloid. The amount of $MV^{+\bullet}$ species yielded by repeated irradiation is similar to that obtained in the first run (as shown in Figure S3 of the Supporting Information).

UV irradiation of the hectorite–niobate colloid in the absence of MV^{2+} ions gives information about the stabilization mechanism of the photogenerated electrons in the nanosheets (although this problem has not been fully understood yet). A broad band (with a maximum at around 400 nm) is observed in the UV/Vis spectrum of the MV^{2+}-free sample after irradiation; this signal can be attributed to the conduction-band electrons[26] (Figure S4a, Supporting Information) and is not observed in the absence of propylammonium ions (Figure S4b, Supporting Information). Thus, we presume that the conduction-band electrons are stabilized by the consumption of positive holes during the oxidative decomposition of the propylammonium ions present around the niobate nanosheets. The oxidation product of propylammonium may then act as an oxidant of $MV^{+\bullet}$ species, thus restoring the MV^{2+} ions in the MV/hectorite–niobate colloid. Titanium dioxide has been reported to photocatalytically oxidize alkylammonium ions.[27] Another possible explanation for the existence of stable conduction-band electrons is hole trapping at certain slow surface states of the exfoliated nanosheets. This option is rationalized by the large surface area of the exfoliated nanosheets, where surface hydroxy groups can be transformed into peroxy groups. In this case, $MV^{+\bullet}$ species can be converted into MV^{2+} ions on the oxidized surface site.

In conclusion, we demonstrate that the microdomain structures formed in a double-component colloid—consisting of niobate and clay nanosheets—are effective for the stabilization of charge-separated states generated by the bandgap excitation of niobate and the subsequent electron transfer to MV^{2+}. Morphologically controlled nanoparticles[13,28] and nanosheets[29] with good electronic properties have recently been fabricated. Further precise tuning of the photochemical characteristics may be possible by using these new materials as building units.

Experimental Section

Synthetic hectorite clay (laponite, supplied by Wilbur–Ellis, with an ideal formula of $Si_8Mg_{5.4}Li_{0.4}H_4O_{24}Na_{0.7}$) was dispersed in water and stored for a week to obtain a homogeneous and stable colloid stock of hectorite nanosheets. Single crystals of layered niobate ($K_4Nb_6O_{17}$) were synthesized from a mixture of K_2CO_3 and Nb_2O_5 powders by means of a flux method.[30] The $K_4Nb_6O_{17}$ crystals were kept for a week in an aqueous solution of propylamine hydrochloride (0.2 M, 80 °C) to ensure the exchange of interlayer K^+ ions for propylammonium ions. The obtained colloid was centrifuged to collect the precipitate (containing the nanosheets), which was rinsed with water to remove excess propylammonium chloride ions. This washing process was repeated six times to finally obtain a stable colloid stock containing exfoliated niobate nanosheets (the lateral dimension of the nanosheets obtained with this method was over 1 μm,[24] whereas that of laponite was about 20 nm).[25] The MV/hectorite and MV/niobate colloids were obtained by adding an aqueous solution of methylviologen chloride to the hectorite and niobate colloids (this was done slowly to avoid flocculation), while the MV/hectorite–niobate colloids were produced by simply mixing the MV/hectorite and the niobate colloids.

For UV irradiation and spectroscopic measurements, the colloids were placed in a water-cooled (25 °C) quartz cell (5 mm thickness) capped with a rubber septum. After bubbling the sample with wet N_2 for over 30 min, it was irradiated by a Xe lamp (Ushio SX-UI500XQ). Visible absorption spectra were recorded on a Shimadzu UV-2450 spectrophotometer before and after irradiation. After terminating irradiation, the spectra were measured repeatedly to monitor the time course of [$MV^{+\cdot}$]. SANS measurements were performed with the SANS-J apparatus,[31] which is located at the JRR-3 atomic reactor of the Japan Atomic Energy Agency (JAEA), Tokai-mura, Japan. The measurements were carried out in a 1-mm-thick quartz cell with a two-dimensional ^{3}He detector positioned 10 m away from the sample. The wavelength of the incident neutron beam was 0.65 nm.

Received: November 2, 2006
Revised: February 22, 2007
Published online: April 19, 2007

Keywords: charge separation · colloids · layered compounds · nanosheets · semiconductors

[1] a) M. R. Hoffmann, S. T. Martin, W. Choi, D. W. Bahnemann, *Chem. Rev.* **1995**, *95*, 69; b) A. L. Linsebigler, G. Lu, J. T. Yates, *Chem. Rev.* **1995**, *95*, 735.
[2] a) M. A. Fox, *Top. Curr. Chem.* **1991**, *159*, 67; b) M. Grätzel, *Heterogeneous Photochemical Electron Transfer*, CRC Press, Boca Raton, FL, **1989**.
[3] Y.-M. Tricot, J. Manassen, *J. Phys. Chem.* **1988**, *92*, 5239.
[4] E. Joselevich, I. Willner, *J. Phys. Chem.* **1994**, *98*, 7628.
[5] A. J. Frank, I. Willner, Z. Goren, Y. Degani, *J. Am. Chem. Soc.* **1987**, *109*, 3568.
[6] a) L. A. Vermeulen, M. E. Thompson, *Nature* **1992**, *358*, 656; b) T. Nakato, K. Kuroda, C. Kato, *J. Chem. Soc. Chem. Commun.* **1989**, 1144; c) R. M. Krishna, V. Kurshev, L. Kevan, *Phys. Chem. Chem. Phys.* **1999**, *1*, 2833.
[7] N. Kakegawa, T. Kondo, M. Ogawa, *Langmuir* **2003**, *19*, 3578.
[8] a) R. M. Krishna, A. M. Prakash, L. Kevan, *J. Phys. Chem. B* **2000**, *104*, 1796; b) K. T. Ranjit, J. Y. Bae, Z. Chang, L. Kevan, *J. Phys. Chem. B* **2002**, *106*, 583.
[9] a) W. Sugimoto, O. Terabayashi, Y. Murakami, Y. Takatsu, *J. Mater. Chem.* **2002**, *12*, 3814; b) T. Sasaki, M. Watanabe, *J. Phys. Chem. B* **1997**, *101*, 10159; c) T. Sasaki, S. Nakano, S. Yamauchi, M. Watanabe, *Chem. Mater.* **1997**, *9*, 602; d) N. Miyamoto, H. Yamamoto, R. Kaito, K. Kuroda, *Chem. Commun.* **2002**, 2378; e) M. Fang, C. H. Kim, T. E. Mallouk, *Chem. Mater.* **1999**, *11*, 1519.
[10] a) N. Miyamoto, T. Nakato, *Adv. Mater.* **2002**, *14*, 1267; b) T. Nakato, N. Miyamoto, A. Harada, *Chem. Commun.* **2004**, 78; c) J.-C. P. Gabriel, F. Camerel, B. J. Lemaire, H. Desvaux, P. Davidson, P. Batail, *Nature* **2001**, *413*, 504; d) A. Mourchid, A. Delville, P. Levitz, *Faraday Discuss.* **1995**, *101*, 275.
[11] N. Sakai, Y. Ebina, K. Takada, T. Sasaki, *J. Am. Chem. Soc.* **2004**, *126*, 5851.
[12] a) L. Onsager, *Ann. N. Y. Acad. Sci.* **1949**, *51*, 627; b) F. M. van der Kooij, K. Kassapidou, H. N. W. Lekkerkerker, *Nature* **2000**, *406*, 868.
[13] L. Li, J. Walda, L. Manna, A. P. Alivisatos, *Nano Lett.* **2002**, *2*, 557.
[14] P. N. Pusey, W. van Megen, *Nature* **1986**, *320*, 340.
[15] a) M. Adams, Z. Dogic, S. L. Keller, S. Fraden, *Nature* **1998**, *393*, 349; b) Z. Dogic, D. Frenkel, S. Fraden, *Phys. Rev. E* **2000**, *62*, 3925; c) F. M. van der Kooij, H. N. W. Lekkerkerker, *Langmuir* **2000**, *16*, 10144.
[16] a) I. Grillo, P. Levitz, T. Zemb, *Eur. Phys. J. E* **2001**, *5*, 377; b) I. Grillo, P. Levitz, T. Zemb, *Langmuir* **2000**, *16*, 4830; c) C. Ménager, L. Belloni, V. Cabuil, M. Dubois, T. Gulik-Krzywicki, T. Zemb, *Langmuir* **1996**, *12*, 3516.
[17] N. Miyamoto, T. Nakato, *Langmuir* **2003**, *19*, 8057.
[18] E. M. Kosower, J. L. Cotter, *J. Am. Chem. Soc.* **1964**, *86*, 5524.
[19] a) E. Borgarello, E. Pelizzetti, *J. Chem. Soc. Faraday Trans. 1* **1985**, *81*, 143; b) K. Chandrasekaran, J. K. Thomas, *J. Chem. Soc. Faraday Trans. 1* **1984**, *80*, 1163; c) D. Dung, J. Ramsden, M. Grätzel, *J. Am. Chem. Soc.* **1982**, *104*, 2977.
[20] a) R. E. Sassoon, *J. Am. Chem. Soc.* **1985**, *107*, 6133; b) A. Slama-Schwok, M. Ottolenghi, D. Avnir, *Nature* **1992**, *355*, 240.
[21] T. Nakato, K. Kuroda, C. Kato, *Chem. Mater.* **1992**, *4*, 128.
[22] K. Domen, A. Kudo, M. Shibata, A. Tanaka, K. Maruya, T. Onishi, *J. Chem. Soc. Chem. Commun.* **1986**, 1706.
[23] C. T. Johnston in *Organic Pollutants in the Environment, CMS Workshop Lectures*, *Vol. 8* (Ed.: B. L. Sawhney), Clay Minerals Society, CO, Boulder, **1996**, pp. 2 – 44.
[24] N. Miyamoto, T. Nakato, *J. Phys. Chem. B* **2004**, *108*, 6152.
[25] E. Balnois, S. Durand-Vidal, P. Levitz, *Langmuir* **2003**, *19*, 6633.
[26] Y. Wada, A. Morikawa, *Bull. Chem. Soc. Jpn.* **1987**, *60*, 3509.
[27] S. Kim, W. Choi, *Environ. Sci. Technol.* **2002**, *36*, 2019.
[28] Y. Yin, A. P. Alivisatos, *Nature* **2005**, *437*, 664.
[29] a) T. Sasaki, M. Watanabe, H. Hashizume, H. Yamada, H. Nakazawa, *J. Am. Chem. Soc.* **1996**, *118*, 8329; b) Y. Omomo, T. Sasaki, L. Wang, M. Watanabe, *J. Am. Chem. Soc.* **2003**, *125*, 3568; c) W. Sugimoto, H. Iwata, Y. Yasunaga, Y. Murakami, Y. Takasu, *Angew. Chem.* **2003**, *115*, 4226; *Angew. Chem. Int. Ed.* **2003**, *42*, 4092.
[30] K. Nassau, J. W. Shiever, J. L. Bernstein, *J. Electrochem. Soc.* **1969**, *116*, 348.
[31] S. Koizumi, H. Iwase, J. Suzuki, T. Oku, R. Motokawa, H. Sasao, H. Tanaka, D. Yamaguchi, H. M. Shimizu, T. Hashimoto, *Physica B* **2006**, *385–386*, 1000.

